Fault Detection of Helicopter Gearboxes Using the Multi-Valued Influence Matrix Method

///- ᵒ/

/ :.·/ ·ᵒ

/ · 3𝜕

Hsinyung Chin and Kourosh Danai
University of Massachusetts
Amherst, Massachusetts

and

David G. Lewicki
Propulsion Directorate
U.S. Army Aviation Systems Command
Lewis Research Center
Cleveland, Ohio

March 1993

NASA

US ARMY
AVIATION
SYSTEMS COMMAND
AVIATION R&T ACTIVITY

FAULT DETECTION OF HELICOPTER GEARBOXES USING THE MULTI-VALUED INFLUENCE MATRIX METHOD

Hsinyung Chin and Kourosh Danai
University of Massachusetts
Amherst, Massachusetts 01003

and

David G. Lewicki
Propulsion Directorate
U.S. Army Aviation Systems Command
Lewis Research Center
Cleveland, Ohio 44135

ABSTRACT

In this paper we investigate the effectiveness of a pattern classifying fault detection system that is designed to cope with the variability of fault signatures inherent in helicopter gearboxes. For detection, the measurements are monitored on-line and flagged upon the detection of abnormalities, so that they can be attributed to a faulty or normal case. As such, the detection system is composed of two components, a *quantization matrix* to flag the measurements, and a *mutli-valued influence matrix* (MVIM) that represents the behavior of measurements during normal operation and at fault instances. Both the *quantization matrix* and *influence matrix* are tuned during a training session so as to minimize the error in detection. To demonstrate the effectiveness of this detection system, it was applied to vibration measurements collected from a helicopter gearbox during normal operation and at various fault instances. The results indicate that the MVIM method provides excellent results when the full range of faults effects on the measurements are included in the training set.

1 INTRODUCTION

Helicopter drive trains are significant contributors to both maintenance cost and flight safety incidents. Drive trains comprise almost 30% of maintenance costs and 16% of mechanically related malfunctions that often result in the loss of aircraft (Chin and Danai, 1991). Future helicopters like the COMANCHE and fixed wing aircraft like the ATF require increased levels of mission capability that simply cannot be met without advancing the state of the art in detection, particularly in critical components like the power trains. These detection systems should be reliable so as to avoid unnecessary emergency landings due to false alarms, and should be fast to be applicable on-line.

For fault detection of helicopter power trains, either debris sensors (chip detectors) are used to detect the presence of residues caused by component failures (Collier-March, 1985), or vibration analysis is employed to identify the presence of any abnormalities that may have been resulted from a fault (e.g., Braun, 1986; Kaufman, 1975). Although chip detectors are effective in detecting failures which produce debris, due to their insensitivity to wear-related faults, are not completely reliable. Vibration analysis, on the other hand, is believed to provide a more generic basis for fault detection (e.g., Cempel, 1988; Astridge, 1986). As such, considerable effort has been directed toward the identification of features of vibration that are affected by specific faults (e.g., Pratt, 1986; Mertaugh, 1986), and the development of signal processing techniques that can quantify such features through the parameters they estimate. For example, the crest factor of vibration, which represents the peak-to-rms ratio of vibration, has been shown to increase with localized faults such as tooth cracks (Braun, 1986). For detection purposes, the parameter values (measurements) obtained through signal processing are analyzed for any abnormalities, and flagged once such abnormality is observed. The simplest and most common method of flagging is thresholding the residuals between individual parameters and their normal-mode values (Chow and Willsky, 1984).

The fundamental problem with the current method of fault detection is that it is at the

1

mercy of the flagging operation. Flags can be posted due to noise, causing false alarms, or the effect of faults may not be identified through flagging, so faults may remain undetected. Neither false alarms nor undetected faults are acceptable for helicopter fault detection, as false alarms will result in unnecessary emergency landings, and undetected faults could cause catastrophic failures.

In order to cope with the uncertainty of flagged measurements, pattern classification techniques have been employed (Pau, 1977). Among the various pattern classifiers used for detection, artificial neural nets are the most notable due to their nonparametric nature (independence of the probabilistic structure of the system), and their ability to generate complex decision regions. However, neural nets generally require extensive training to develop the decision regions (detection model). In cases such as helicopter power trains, where adequate data is usually not available for training, artificial neural nets are known to also produce false alarms or leave faults undetected.

The purpose of this paper is to investigate the applicability of the MVIM method (Danai and Chin, 1991) in helicopter power train fault detection. This method uses nonparametric pattern classification to estimate its detection model, so like artificial neural nets it is independent of the probabilistic structure of the system. Furthermore, since this method benefits from an efficient learning algorithm based on detection error feedback, it can estimate its detection model based on a small number of measurement-fault data. This method utilizes a two-column *multi-valued influence matrix (MVIM)* as its detection model to represent no-fault and fault signatures, and relies on a simple detection strategy which makes it suitable for on-line detection. The MVIM method can also assess the significance of individual parameters in detection based on their influence on the speed of training of the system.

To train and test the MVIM, vibration data reflecting the effect of various helicopter main rotor transmission faults were obtained from NASA. This vibration data was then processed through a microcomputer customized for vibration signal processing, so that the obtained pa-

2

rameters can be utilized to train the MVIM method and test its performance. Detection results indicate that the MVIM method produces perfect detection when trained with the full range of fault effects on the parameters, and that it produces better overall detection than a neural net using error back-propagation learning algorithm trained and tested with the same data sets. The MVIM method is also utilized to rank the parameters for their significance in detection. It is shown that through this ranking procedure the optimal subset of parameters for detection can be selected, which is particularly important in reducing processing time for on-line detection purposes.

2 EXPERIMENTAL

Vibration data was collected at NASA Lewis Research Center as part of a joint NASA/Navy/Army Advanced Lubricants Program to reflect the effect of various faults in an OH-58A main rotor transmission (Lewicki et al., 1992). The configuration of the transmission which was tested in the NASA 500-hp Helicopter Transmission Test Stand is shown in Fig. 1. The vibration signals were measured by eight piezoelectric accelerometers (frequency range of up to 10 KHz), and an FM tape recorder was used to record the signals periodically once every hour, for about one to two minutes per recording (at the tape speed of 30 in/sec, providing a bandwidth of 20 KHz). Two chip detectors were also mounted inside the transmission to detect the residues caused by component failures. The location and orientation of the accelerometers are shown in Fig. 2, and the schematic of the vibration recording/monitoring system is shown in Fig. 3.

In these experiments, failures occurred naturally. The transmission was run under a constant load and was disassembled/checked periodically or when one of the chip detectors indicated a failure. A total of five tests were performed, where each test was run between nine to fifteen days for approximately four to eight hours a day. Among the eight failures occurred during these tests (see Table 1), there were three cases of planet bearing failure, three cases of sun
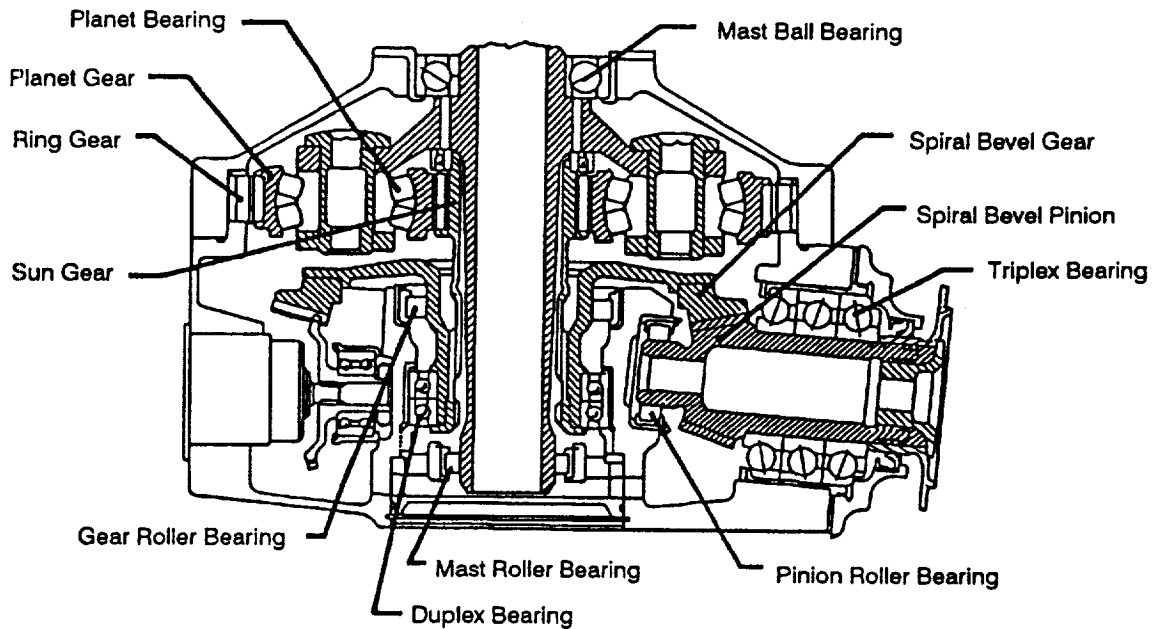
Figure 1.—Configuration of the OH-58A main rotor transmission.

gear failure, two cases of top housing cover crack, and one case each of spiral bevel pinion, mast bearing, and planet gear failure. Insofar as fault detection during these tests, the chip detectors were reliable in detecting failures in which a significant amount of debris was generated, such as the planet bearing failures and one sun gear failure. The remaining failures were detected during routine disassembly and inspection. Vibration monitoring during testing was not used as a diagnostic tool.

3 SIGNAL PROCESSING

In order to identify the effect of faults on the vibration data, the vibration signals obtained from the five tests were digitized and processed by a commercially available diagnostic ana-

4

#1, 2, 3 attached to block on right trunnion mount
#4, 6, 7, 8 studded to housing through steel inserts
#5 attached to block on input housing

Left trunnion mount

7

Transverse

Longitudinal

4 **6**

8

1

Right trunnion mount

Transmission output

3

2

Vertical
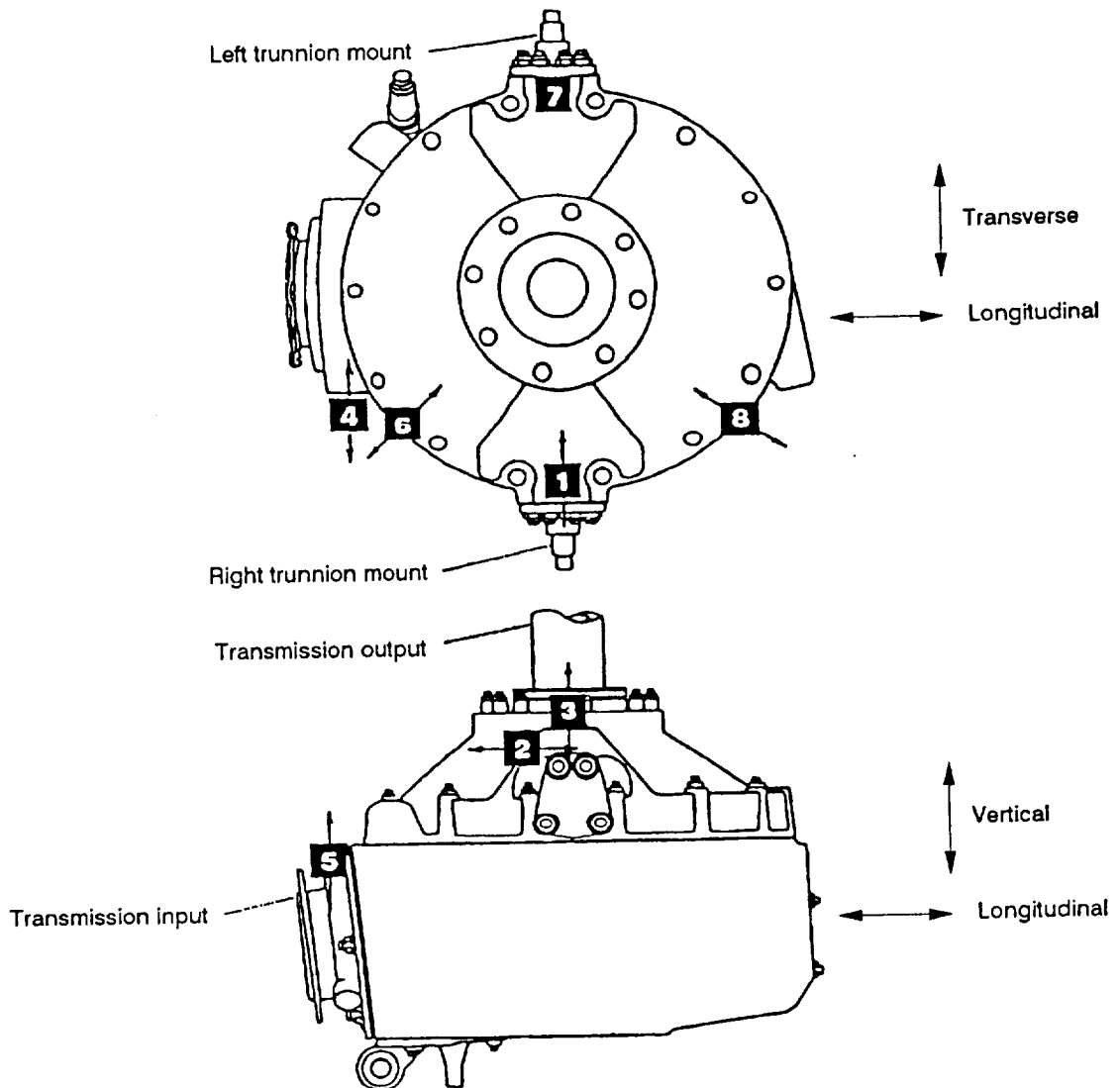
5

Longitudinal

Transmission input

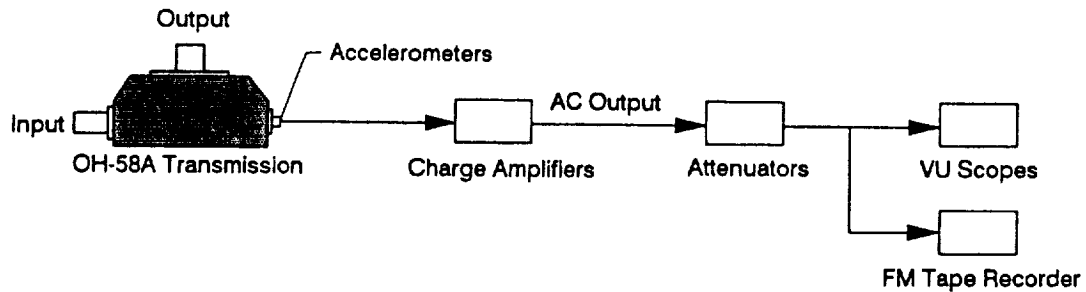Figure 2.—Location of the accelerometers on the test stand.

Figure 3.—Schematic of vibration recording/monitoring.

lyzer (Stewart Hughes Limited, 1986). Three processing modules of the analyzer were used:
1) *Statistical Analysis (STAT)*, 2) *Baseband Power Spectrum Analysis (BBPS)*, and 3) *Bearing Analysis (BRGA)*. For analysis purposes, only one data record per day was used for each test. These data records were taken at the beginning of the day unless a fault was reported, which in that case, the record taken right before the fault incident was selected to ensure that the data record reflected the fault. Also, in order to reduce estimation errors, each data record was partitioned into sixteen segments and parameters were estimated for each segment and averaged over these segments. The data records as well as the parameters obtained from the above processing modules were then transferred to a personal computer for further analysis. The schematic of the data acquisition apparatus and the parameters obtained from each module of the diagnostic analyzer are illustrated in Fig. 4. Note that the objective of this paper is to demonstrate the MVIM pattern classification scheme, not to develop/verify individual diagnostic algorithms. The algorithms described in the next subsections were used to determine inputs to the MVIM method, but may not be optimized for transmission health monitoring.

6

Test #	Number of Days	Failures
1	9	Sun gear tooth pit Spiral bevel pinion scoring/heavy wear
2	9	None
3	13	Planet bearing #2 inner race spall Top cover housing crack Planet bearing #2 inner race spall Micropitting on mast bearing
4	15	Planet bearing #3 inner race spall Sun gear tooth pit
5	11	Sun gear teeth spalls Planet gear tooth spall Top housing cover crack

Table 1: Faults occurred during the experiments.

3.1 Statistical Analysis

It is generally believed that the probability density function (p.d.f.) of the vibration amplitude is near Gaussian when machinery is healthy, and that its shape changes when a defect appears. The *Statistical Analysis Module* of the diagnostic analyzer estimates parameters that would characterize such change. Among the parameters available from this module, the skewness, kurtosis, crest factor, and peak-to-peak value of vibration data are reported to be good indicators of localized defects in rotating machinery (e.g., see Dyer and Stewart, 1978). A brief description of these parameters is as follows:

- **Skewness Coefficient.** The skewness coefficient represents the symmetry of probability density function of the vibration amplitude. Since the skewness coefficient of a Gaussian distribution is zero, any deviations of the skewness coefficient from zero can be due to failure.

- **Kurtosis Value.** The kurtosis value, which represents the concentration of heights around the mean line of the probability density function, is equal to 3 for a Gaussian distribution. As such, kurtosis values larger than 3 are reported to be indicators of localized defects (Dyer

and Stewart, 1978).

- **Crest Factor.** Similar to the kurtosis value, the crest factor is used to describe the 'peakness' of the probability density function (Braun, 1986). However, unlike the kurtosis value, the crest factor is only a relative measure. Moreover, since the crest factor is more likely to be affected by a single outlier, it is generally not as robust as the kurtosis value.

- **Peak-to-Peak Value.** When failures occur, the amplitude of the vibration tends to increase in both upward and downward directions and thus the peak-to-peak value is expected to increase.

The above statistical parameters were obtained for the five tests. The results indicate that none of the parameters provide a good indication of all the faults. For example, the averaged kurtosis values of the vibration signals from the eight accelerometers are shown in Fig. 5 for the five tests. The results indicate that the kurtosis value reflects only the fault incident at the end of Test #5, and that it is not sensitive to the other six fault incidents in the other tests (marked by asterisks). The significant increase in the kurtosis value at the end of Test #5 is perhaps caused by the severity of faults in this test (i.e., sun gear teeth spall, planet tooth spall, and top housing crack).
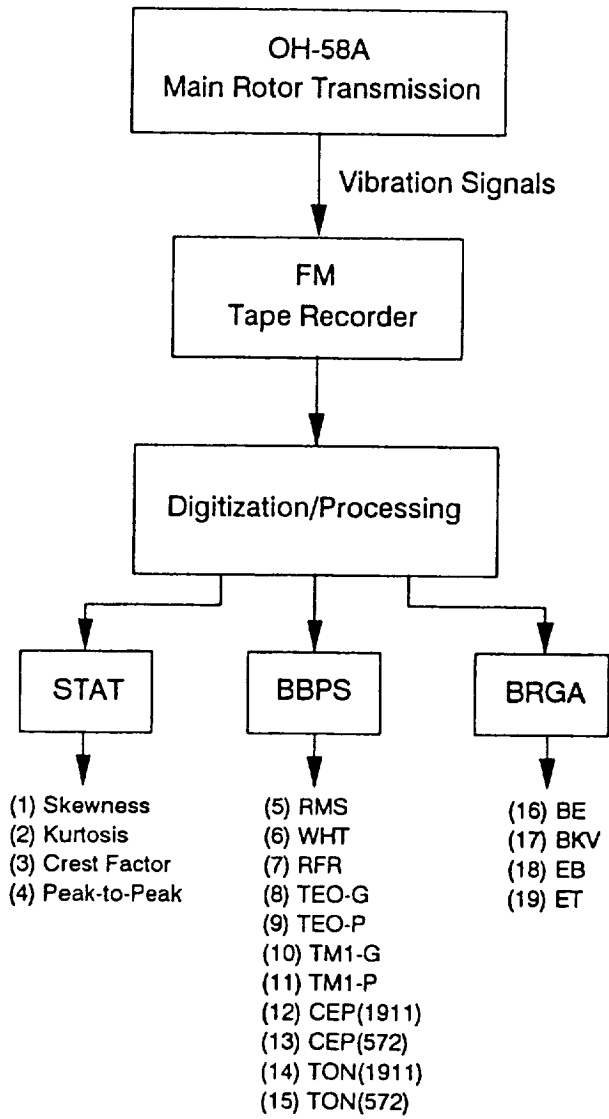
Figure 4.—Schematic of the data acquisition apparatus, as well as the parameters obtained from the diagnostic analyzer.
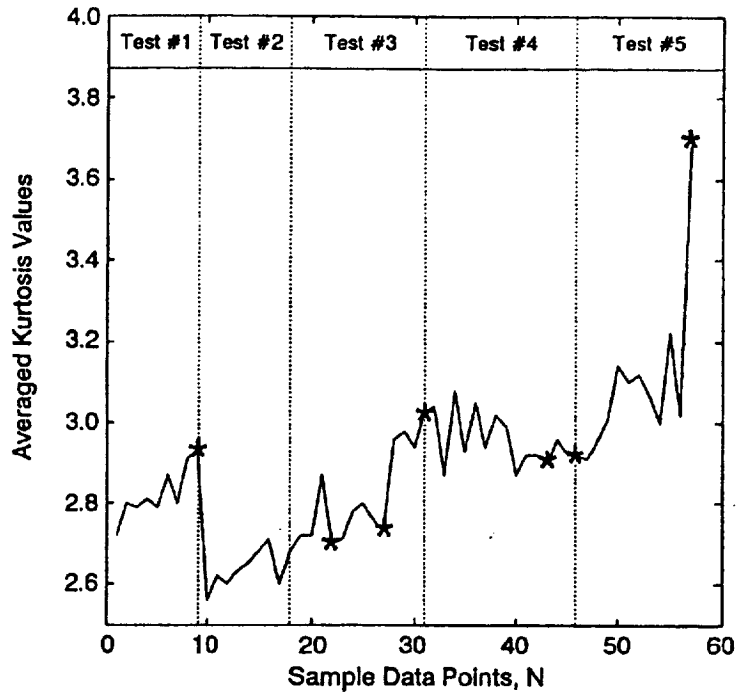
Figure 5.—Averaged kurtosis values for the five tests from the
Statistical Analysis Module. Faults are indicated by asterisks.

3.2 Baseband Power Spectrum Analysis

Spectrum analysis (or frequency domain analysis) is perhaps the most widely used technique in vibration signal processing, as failures such as unbalance, misalignment, wear, and roller bearing spalling produce a clear change in the spectrum (e.g., see Dewell and Mitchell, 1984; Randall, 1982; Taylor, 1980; Lees and Pandey, 1980). However, in complex machinery where the background noise masks the basic distress signal, changes in the spectra cannot be easily distinguished (Pratt, 1986). The *Baseband Power Spectrum Analysis Module* provides several parameters that can be associated with the frequencies generated by individual components of the transmission. The parameters obtained from this module are:

10

- **Root-Mean-Square.** The root-mean-square (RMS) value of the vibration amplitude represents the overall energy level of vibrations. As such, the RMS value can be used to detect major changes in the vibration level.

- **White Spectrum.** The white spectrum (WHT) represents the rms level of the signal minus its strong tones. Therefore, it denotes the energy level in the base of the spectrum. Since certain failures, like wear, do not seem to increase the strong tones created by shaft rotation and gear mesh, the energy in the base of the spectrum could potentially be a powerful detection parameter for wear-related failures.

- **Rice Frequency.** The rice frequency (RFR) denotes the position of the 'center of gravity' of the spectrum. Therefore, it can reflect any major changes in the shape of the spectrum that may have been caused by faults.

- **Comparison Analysis.** Failures in rotating machinery tend to increase spectral levels. The *Comparison Analysis Function* provides several statistical parameters about the spectral ratio between the current spectrum and a baseline spectrum. The baseline spectrum could either be the spectrum of vibration at the beginning of the test (TEO) or the spectrum of vibration from the previous record (TM1). Among the statistical parameters obtained from this function, TEO-G and TEO-P, which denote the energy level (rms) and the mean value, respectively, of the spectral ratio with respect to the first spectrum, and TM1-G and TM1-P, which represent the energy level (rms) and the mean value, respectively, of the spectral ratio with respect to the preceding spectrum, are particularly effective in representing differences between the current and the baseline spectrum.

- **Metacepstral Analysis.** The *Metacepstrum Analysis Function* is used to detect the periodic features of the vibration signal (Lyon and Ordubadi, 1982; Childers et al., 1977). The parameters obtained from this function are measures of the energy level at a given frequency and its harmonics. The two frequencies selected for this analysis were the

toothmeshing frequency of the spiral bevel mesh (1911 Hz) and the toothmeshing frequency of the planetary mesh (572 Hz). The parameters calculated for these two frequencies are represented as CEP(1911) and CEP(572).

- **Tone Analysis.** The energy level associated with a particular tone within a spectrum is also a good indicator of faults. Various faults like unbalance and misalignment tend to increase the tone energy. The two parameters TON(1911) and TON(572) obtained for this analysis represent the tone energies at 1911 Hz and 572 Hz, respectively.

The above parameters from the *Baseband Power Spectrum Analysis Module* were computed for the five tests. The results indicate that although some of these parameters are good indicators of specific faults, they are also prone to false alarms. For example, the averaged TM1-G values of the vibration signals, from the eight accelerometers, obtained for the five tests are shown in Fig. 6. The results indicate that while this parameter is sensitive to one of the faults in Test #3 (i.e., the first fault caused by planet bearing inner race spall), it also contains a spike on day 5 of Test #1 which could result in a false alarm.

3.3   Bearing Analysis

The vibration energy of bearing elements is usually lower than those produced by gears, shafts, and sometimes noise. As such, bearing faults cannot be readily detected through abnormalities in the bearing tone. However, since bearing faults such as spalling produce time domain impulses which modulate the bearing shaft frequency over a wide range of frequencies, there are features of high frequency vibration that would reflect such bearing faults (Mathew and Alfredson, 1984; Braun and Datner, 1979). The *Bearing Analysis Module* is designed to extract such features. This module uses a *heterodyner* to demodulate the vibration signals and obtain an amplitude envelope (e.g., see Courrech and Gaudet, 1985), and then calculates the power spectrum of this envelope (i.e., spectral envelope) so that its various features (parameters) can be estimated for
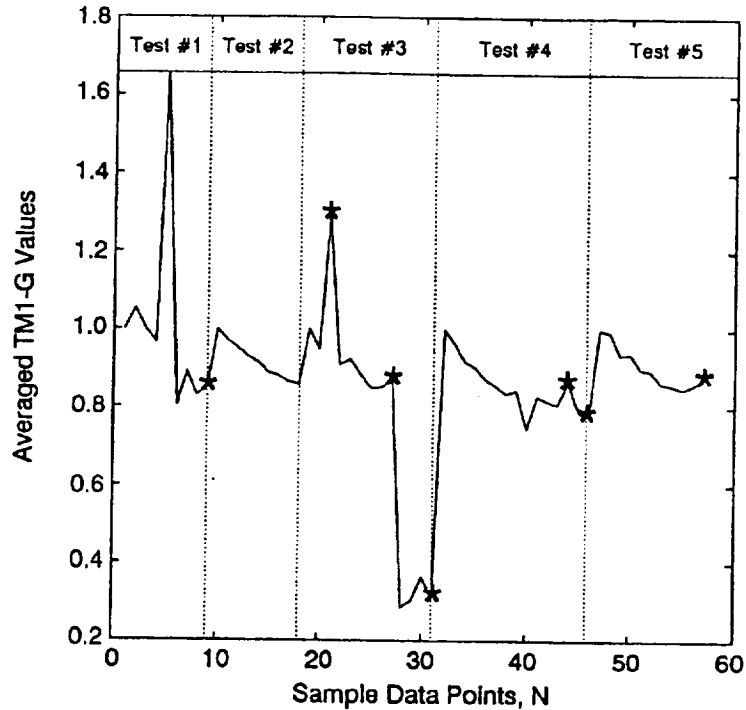
Figure 6.—Averaged TMI-G values for the five tests obtained from the Base-band Power Spectrum Analysis Module. Faults are indicated by asterisks.

bearing fault detection (Dyer and Stewart, 1978; Yhland and Johansson, 1970). The parameters obtained from this module are:

- **Envelope Band Energy.** The band energy (BE), which is calculated as the sum of the mean and standard deviation of the full bandwidth envelope, represents the overall energy level of the envelope. This parameter is expected to be sensitive to most bearing faults which increase the level of vibration.

- **Envelope Kurtosis Value.** The kurtosis value of the envelope (BKV) is estimated to reflect impulsive behavior of vibrations produced by localized bearing faults.

- **Envelope Base Energy.** The envelope base energy (EB) represents the base energy of the spectrum after all tones have been removed. This parameter is expected to reflect

heavy bearing damage.

- **Envelope Tone Energy.** The tone energy (ET) represents the total energy minus the base energy. This parameter is expected to reflect localized bearing faults.

The above parameters from the *Bearing Analysis Module* were computed for the five tests. The results indicate that most of the parameters are not very sensitive to the faults occurred during the tests. For example, the averaged values of the kurtosis value of the envelope (BKV) are shown in Fig. 7. The results indicate that while the BKV is relatively sensitive to the faults in Tests #1 and #3, it exhibits a spike in Test #3 which could potentially result in a false alarm.
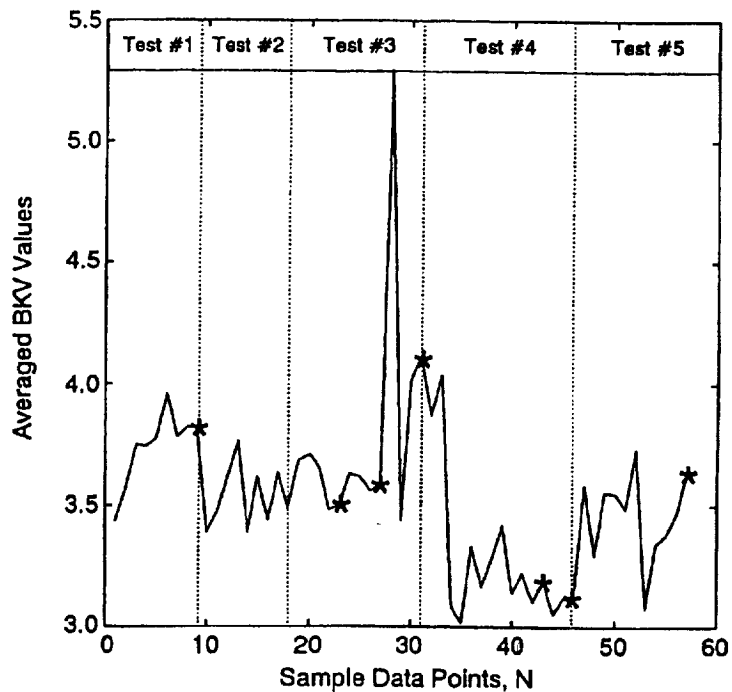
Figure 7.—Averaged BKV values of the envelope kurtosis values for five tests. Faults are indicated by asterisks.

4 THE MVIM METHOD

The MVIM method is based on a *multi-valued influence matrix* (MVIM) which represents the uncertain relationship between various faults and measurements (Danai and Chin, 1991). Measurements in this method are monitored in-process and converted to binary numbers through *flagging* (see Fig. 8), which are posted in a vector of 'flagged measurements'. Flagging in this method is performed by a *quantization matrix*, and detection is performed by matching this vector of flagged measurements against the individual columns of the influence matrix (influence vectors). Influence vectors which represent the *no-fault signature* and the *fault signature* are continuously updated by a learning algorithm to improve detection.

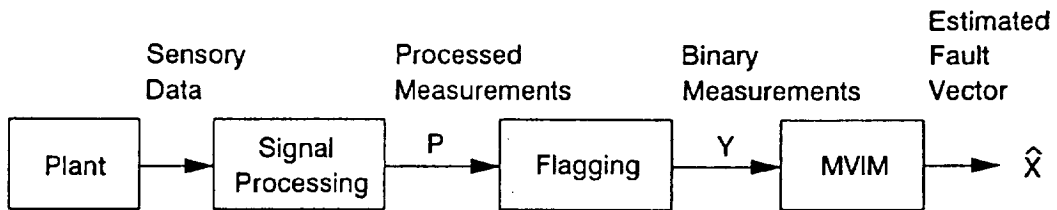Figure 8.—Detection strategy in the MVIM method.

4.1 Detection Model

The multi-valued influence matrix **A** representing the *no-fault signature* and *fault signature* is defined as

$$\mathbf{Y}(t) \stackrel{\mathbf{A}}{\Longleftrightarrow} \mathbf{X}(t) \tag{1}$$

to relate the *flagged measurement vector* $\mathbf{Y}(t)$:

$$\mathbf{Y}(t) = \{y_1(t),\ y_2(t),\ \dots,\ y_m(t)\}^T \tag{2}$$

15

to the fault vector $X(t)$:

$$X(t) = \{x_1(t), \ x_2(t)\}^T \tag{3}$$

where m is the number of measurements. In the above equations, the vectors Y and X are binary vectors; i.e., the y_i (individual flagged measurements) and x_i (the no-fault variable x_1 and the fault variable x_2) can only be equal to 0 or 1, representing the status of the particular measurement and fault at the time, respectively. Note that the the components of the $(m \times 2)$ influence matrix A in Eq. (1), which represents a functional mapping between Y and X, are between 0 and 1 defining the causal relationship between individual flagged measurements y_i and the no-fault and fault cases. For example, an $a_{12} = 0.8$ implies that the possibility of the 1st measurement being flagged at the instance of fault is 0.8, or an $a_{31} = 0.2$ indicates that a 0.2 possibility exists that the 3rd measurement is flagged for a no-fault case.

4.2 Detection

Detection in the MVIM method is based on matching the vector of flagged measurements against the individual influence vectors. The closeness of vectors in the MVIM method is based on their orientation. Accordingly, the possibility of occurrence (*diagnostic certainty measure*) of the no-fault or fault case is defined as the cosine of the angle between the corresponding influence vector and the vector of flagged measurements. The geometric representation of this reasoning, for a three dimensional measurement vector ($m = 3$), is illustrated in Fig. 9. Vectors V_1 and V_2 in this figure represent the influence vectors associated with the no-fault and fault case, respectively, and vector Y denotes the vector of flagged measurements.

In the MVIM method, the vector of *diagnostic certainty measures* which ranks the variables x_1 and x_2 for their possibility of occurrence is defined as

$$\hat{X} = \left\{ \begin{array}{c} \hat{x}_1 \\ \hat{x}_2 \end{array} \right\} = \left\{ \begin{array}{c} \cos\alpha_1 \\ \cos\alpha_2 \end{array} \right\} = \left\{ \begin{array}{c} \bar{V}_1^T \bar{Y} \\ \bar{V}_2^T \bar{Y} \end{array} \right\} \tag{4}$$

where α_1 and α_2 denote the angles between the influence vectors V_1 and V_2, respectively, and
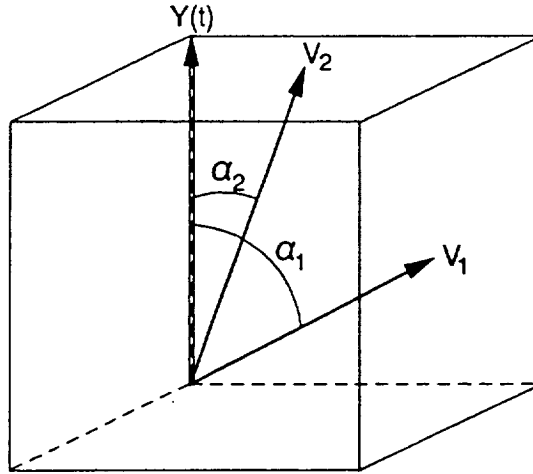
16

Figure 9.—Geometric representation of diagnostic reasoning in the MVIM method for a three dimensional case.

the flagged measurement vector $\mathbf{Y}$, and $\bar{\mathbf{V}}_j$ ($j = 1, 2$) and $\bar{\mathbf{Y}}$ are the normalized forms of vectors $\mathbf{V}_j$ and $\mathbf{Y}$, respectively, defined as

$$\bar{\mathbf{V}}_j = \frac{\mathbf{V}_j}{\|\mathbf{V}_j\|} = \left\{ \frac{a_{ij}}{\sqrt{\sum_{i=1}^{m} a_{ij}^2}} \right\} \tag{5}$$

and

$$\bar{\mathbf{Y}} = \frac{\mathbf{Y}}{\|\mathbf{Y}\|} = \left\{ \frac{y_i}{\sqrt{\sum_{i=1}^{m} y_i^2}} \right\} . \tag{6}$$

Detection in the MVIM method is based on obtaining the vector of diagnostic certainty measures $\hat{\mathbf{X}}$. To obtain $\hat{\mathbf{X}}$, however, the normalized form of the influence matrix, $\bar{\mathbf{A}}$,

$$\bar{\mathbf{A}} = \begin{bmatrix} \bar{\mathbf{V}}_1 & \bar{\mathbf{V}}_2 \end{bmatrix}$$

is required. Since this matrix is not known *a priori*, it will have to be estimated.

4.3 Estimation of $\bar{A}$

One of the main features of the MVIM method is its capability to use the detection error as feedback in estimating/updating $\bar{A}$. Based on this learning strategy, individual columns of the influence matrix are adjusted recursively after the occurrence of fault, or when a flag is posted in a no-fault case, to minimize the sum of the squared detection error. The estimation algorithm of $\bar{A}$ which is based on recursive least-squares estimation (Ljung, 1987) is given in (Danai and Chin, 1991), where its performance is demonstrated in simulation.

4.4 Flagging

In the MVIM detection system, flagging of measurements is performed by a *quantization matrix*. For flagging, the measurements P are multiplied by the weights of the *quantization matrix* Q

$$Q = [W_1 \quad \ldots \quad W_i \quad \ldots \quad W_m] \; , \tag{7}$$

and hard-limited as

$$y_i = \begin{cases} 1 & \text{when } P^T W_i \geq 0.5 \\ 0 & \text{otherwise} \end{cases} \tag{8}$$

to produce the binary vector of flagged measurements Y (see Fig. 10). This vector is used for both detection, as well as estimating/updating the MVIM. The vectors W_i in Eqs. (7) and (8) represent the columns of the *quantization matrix* associated with individual measurements.

The vectors of the MVIM are trained based on the flagged measurements y_i (see Eq. (8)). Therefore, they are directly influenced by the flagging operation. In order to improve the flagging operation, the *quantization matrix* is adapted during a training session. Ideally, we would like the magnitude of all flagged measurements y_i to be equal to 0 for no-fault cases and 1 at fault instances. Therefore, the components of the *quantization matrix* are adjusted to produce such ideal flagged measurement vectors (see Fig. 10).

The proposed *quantization matrix* uses a sample set of measurement-fault vectors to tune
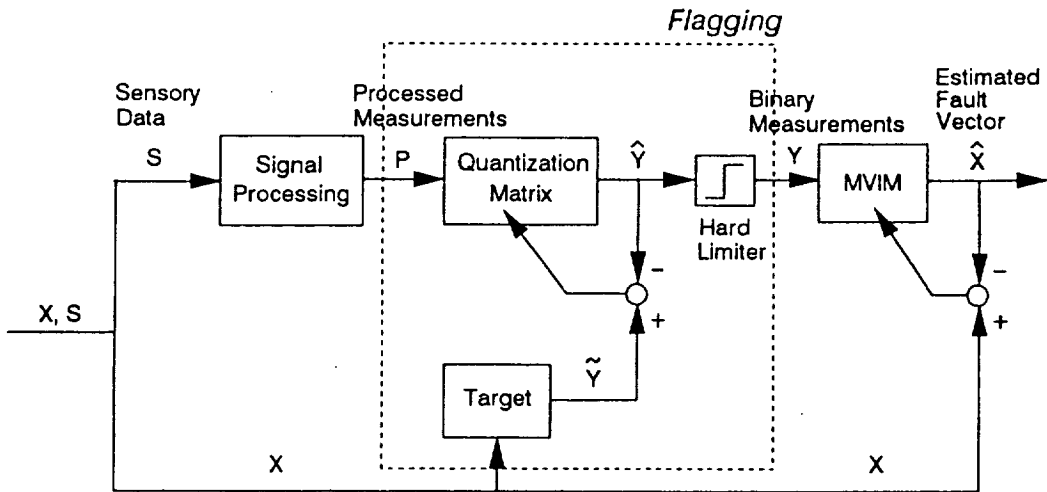
18

Figure 10.—Schematic diagram of adaptation in the MVIM method.

its parameters iteratively. For this purpose, it uses recursive least-squares adaptation to min-imize the sum of square errors between the individual flagged measurements produced by the *quantization matrix* and their ideal values. This learning algorithm has the form

$$w_{ij}(\mu) = w_{ij}(\mu - 1) + l_j(\mu - 1) \left[\tilde{y}_i(\mu) - \mathbf{P}^T(\mu)\mathbf{W}_i(\mu - 1)\right] \tag{9}$$

where the w_{ij} denote the components of the *quantization matrix*, μ is the iteration step, $\tilde{y}_i$ represent the ideal value of flagged measurements (i.e., $\tilde{y}_i = 1$ for fault cases, and $\tilde{y}_i = 0$ for no-fault cases), and the l_j denote the components of the adaptation gain vector $\mathbf{L}$, updated according to the relationship (Ljung, 1987)

$$\mathbf{L}(\mu) = \frac{\mathbf{R}(\mu - 1)\mathbf{P}^T(\mu)}{1 + \mathbf{P}(\mu)\mathbf{R}(\mu - 1)\mathbf{P}^T(\mu)} \tag{10}$$

where matrix $\mathbf{R}$ denotes the covariance matrix in least-squares estimation computed as

$$\mathbf{R}(\mu) = \mathbf{R}(\mu - 1) - \mathbf{L}(\mu)\mathbf{P}(\mu)\mathbf{R}(\mu - 1). \tag{11}$$

19

5 DETECTION RESULTS

The averaged values of the nineteen parameters obtained from the diagnostic analyzer were used as the components of the measurement vector $\mathbf{P}$ to train and test the MVIM (see Figs. 4 and 10). For scaling purposes, each parameter value was normalized with respect to the value of the parameter on the first day of each test.

As explained in the previous section, the MVIM method requires a set of measurements during normal operation and at fault incidents to estimate the no-fault and fault signatures. Since in the experiments the exact time of fault was not known, the time of fault occurrence was conservatively set on the last day, or right before failure was verified through disassembly. Similarly, no-fault cases were assumed only for the first day of each test, and after faulty components were replaced. The specification of vibration data as fault and no-fault on various days of each test are listed in Table 2. For Tests #1 and #5, only the data from the last day (day 9 and day 11, respectively) was associated with a fault case, since faults in these tests were only found on the last day during routine disassembly. For Test #2, the data from all of the nine days were marked as no-fault, since no faults were detected during inspection at the end of the ninth days. For Test #3, the data from days 1, 5, and 10 were associated with a no-fault case, because they were obtained directly after faulty components were replaced on days 4, 9, and 13. For Test #4, data from days 1–8 was attributed to a no-fault case, since no faults were detected upon inspection at the end of the eighth day. For this test, the data from days 12 and 15, which were collected before faulty components were replaced, were associated with fault incidents. Note that the data from day 13, obtained directly after the replacement of the faulty component, is also associated with a no-fault case.

The effectiveness of the MVIM detection method was evaluated with different training sets.

Day	Fault Status				
	Test #1	Test #2	Test #3	Test #4	Test #5
1	no-fault	no-fault	no-fault	no-fault	no-fault
2	-	no-fault	-	no-fault	-
3	-	no-fault	-	no-fault	-
4	-	no-fault	fault	no-fault	-
5	-	no-fault	no-fault	no-fault	-
6	-	no-fault	-	no-fault	-
7	-	no-fault	-	no-fault	-
8	-	no-fault	-	no-fault	-
9	fault	no-fault	fault	no-fault	-
10			no-fault	-	-
11			-	-	fault
12			-	fault	
13			fault	no-fault	
14				-	
15				fault	

Table 2: Association of data from each day of the 5 tests with fault and no-fault cases. The mark '-' denotes that data from that day cannot be specified.

For this purpose, training sets were formed based on parameters from various combinations of five tests (see Table 3). For each training case, the initial values of the MVIM (19×2) and the quantization matrix (19×19) were set to 0 and I, respectively, and training was continued until perfect detection was achieved in the training set (i.e., no false alarm or undetected fault was found in the training set). The MVIM was then tested on all the data from all of the five tests. Performance of the MVIM was represented by the total number of false alarms and undetected faults it produced during testing (denoted as Total Test Errors in Table 3). The detection results produced by the MVIM for 30 different cases of training are shown in Table 3.

For comparison purposes, the results obtained from the MVIM are contrasted against the results obtained from a multi-layer neural net (e.g., see Hertz et al., 1991; Rumelhart et al., 1988) which was trained and tested under the same conditions. The neural net was trained with the back-propagation learning algorithm and contained 40 hidden units. This number of hidden units was selected within a range of 30 to 50 hidden units to optimize its generalization

ability. For training the net, the learning rate and momentum coefficient were set at 0.2 and 0.8, respectively. The above parameters were selected within a range of 0.2 to 0.8 through trial and error so as to optimize the convergence speed of the net.

The results in Table 3 indicate that the MVIM was able to provide perfect detection when faults were fully represented by the training sets (i.e., Cases #18, #21, #24, #25, #28, #29, and #30), and that it produced better results than the neural net in most of the cases. Specifically, the MVIM produced better results in nineteen of the test cases, produced identical results in ten cases, and was outperformed in only one case. Upon a casual inspection of the training sets that enabled MVIM to perform perfect detection, it can be observed that Tests #3 and #4 are included in all of them. This implies that the MVIM needs the parameters from these two tests to establish an effective pair of signatures for no-fault and fault cases. Note that without Test #3, the MVIM produces one undetected fault and one false alarm (Case #27), and without Test #4 it produces one undetected fault (Case #28). Note that the multi-layer neural net could not provide perfect detection even when trained with all of the five tests (Case #30).

Case #	Training Data Sets	Diagnostic Method	Undetected Faults	False Alarms	Total Test Errors
1	1	Neural Net	4	0	4
		MVIM	1	3	4
2	3	Neural Net	1	3	4
		MVIM	1	1	2
3	4	Neural Net	5	1	6
		MVIM	2	1	3
4	5	Neural Net	1	2	3
		MVIM	3	2	5
5	1,2	Neural Net	4	0	4
		MVIM	2	2	4
6	1,3	Neural Net	1	2	3
		MVIM	2	0	2
7	1,4	Neural Net	1	1	2
		MVIM	1	1	2
8	1,5	Neural Net	1	2	3
		MVIM	1	2	3
9	2,3	Neural Net	1	1	2
		MVIM	1	1	2
10	2,4	Neural Net	4	2	6
		MVIM	3	1	4
11	2,5	Neural Net	3	2	5
		MVIM	3	2	5
12	3,4	Neural Net	2	2	4
		MVIM	0	0	0
13	3,5	Neural Net	0	3	3
		MVIM	1	0	1
14	4,5	Neural Net	3	0	3
		MVIM	1	1	2
15	1,2,3	Neural Net	1	2	3
		MVIM	2	0	2
16	1,2,4	Neural Net	2	1	3
		MVIM	2	1	3
17	1,2,5	Neural Net	1	2	3
		MVIM	1	2	3
18	1,3,4	Neural Net	1	0	1
		MVIM	0	0	0
19	1,3,5	Neural Net	0	3	3
		MVIM	2	0	2
20	1,4,5	Neural Net	1	1	2
		MVIM	1	1	2

Case #	Training Data Sets	Diagnostic Method	Undetected Faults	False Alarms	Total Test Errors
21	2,3,4	Neural Net	2	0	2
		MVIM	0	0	0
22	2,3,5	Neural Net	1	2	3
		MVIM	1	0	1
23	2,4,5	Neural Net	3	1	4
		MVIM	1	1	2
24	3,4,5	Neural Net	2	0	2
		MVIM	0	0	0
25	1,2,3,4	Neural Net	2	0	2
		MVIM	0	0	0
26	1,2,3,5	Neural Net	2	1	3
		MVIM	1	0	1
27	1,2,4,5	Neural Net	1	1	2
		MVIM	1	1	2
28	1,3,4,5	Neural Net	1	0	1
		MVIM	0	0	0
29	2,3,4,5	Neural Net	2	0	2
		MVIM	0	0	0
30	1,2,3,4,5	Neural Net	1	0	1
		MVIM	0	0	0

Table 3: Detection results obtained from MVIM and a multi-layer neural net when trained with different data sets.

6 MEASUREMENT SELECTION

The MVIM method can also assess the significance of individual parameters in detection. It is generally assumed that the parameters which reflect the faults more effectively facilitate training, particularly when the success of training is based upon detection capability within the training set. Therefore, when individual parameters are discarded, their influence on overall detectability must be reflected in the training time for that set. This means that when an 'important' parameter (measurement) is discarded from the training set, for the faults are to be characterized by the remaining parameters (measurements), the training will be more difficult and, thus, more time-consuming.

In order to test the above hypothesis, a training set which provided perfect detection results was selected. Among the various training sets in Table 3 satisfying this condition, Case #12 which contained the smallest number of data sets (i.e., Tests #3 and #4) was selected. Individual parameters were then discarded one at a time from this training set to form new reduced sets for training the MVIM. The number of training epochs[1] required for each reduced set is shown in Table 4, with the discarded parameters imposing higher than 9 epochs (obtained for the full set) marked by a plus sign.

Case # 12 (Test # 3 and #4)			
Parameter Discarded	Number of Training Epochs	Undetected Faults	False Alarms
None	**9**	**0**	**0**
#1	9	0	0
#2	9	0	0
#3+	25	0	0
#4	9	0	0
#5	9	0	0
#6	9	0	0
#7	8	0	0
#8	9	0	0
#9	9	0	0
#10	9	0	0
#11+	10	0	0
#12+	100*	0	6
#13+	11	0	0
#14+	10	0	0
#15+	37	0	0
#16+	10	0	0
#17+	22	0	2
#18	8	0	0
#19	9	0	0

Table 4: The effect of discarded parameters on training time and test results. The particular sets that required a longer training time than the full set are marked by '+'. The '*' denotes that full detection within the training set was never achieved.

---

[1] passes through the training set

Based on the results in Table 4, the elimination of Parameters #3 (crest factor), #11 (TM1-P), #12 (CEP(1911)), #13 (CEP(572)), #14 (TON(1911)), #15 (TON(572)), #16 (BE), and #17 (BKV) from the training set adversely affected training. This could imply that these eight parameters are particularly important in characterizing the signatures for the no-fault and fault case, and that Parameter #12, whose elimination jeopardized training, is critical. By the same analogy, the results in Table 4 indicate that discarding Parameters #7 and #18 may be even beneficial to training of MVIM.

In order to validate the above findings, various combinations of parameters from Tests #3 and #4 were grouped into training subsets. Training started with the smallest possible subset which included only two parameters. As the MVIM did not converge with this subset, the subset was expanded further until successful training was obtained for the MVIM. The first subset that resulted in perfect training for the MVIM was one with twelve parameters, of which eight parameters were those that were identified as 'important' before (i.e., Parameters #3, #11, #12, #13, #14, #15, #16, and #17). In fact, through further analysis it was ascertained that the smallest subset of parameters that would provide perfect training for the MVIM consists of these eight parameters, and that discarding or replacing any of these eight parameters results in a non-trainable situation. Addition of more parameters to this subset did not make a difference.

The same type of analysis performed with the MVIM method could potentially be performed with a neural net. However, neural nets provide different detection results with different number of hidden units. As such, for each number of inputs (parameters) the optimal number of hidden units need to be selected, which would then affect the number of epochs required for training. This will complicate the criteria for measurement selection of the type described above. The advantage of the MVIM method over a neural net is that its structure is fixed based on the number of its inputs, and thus the number of training epochs would directly reflect the significance of individual measurements.

7 CONCLUSION

Fault detection of helicopter power transmissions through pattern classification is demonstrated. For this purpose, the MVIM detection method is used to construct no-fault and fault signatures based on vibration data reflecting the effect of various faults in an OH-58A main rotor transmission. Implementation results indicate that the MVIM can provide perfect detection when the full range of fault effects are extracted through appropriate signal processing. The MVIM method can also assess the significance of individual measurements. Based on this assessment, it is shown that an optimal subset of measurements can be selected so as to reduce processing time for in-flight implementation purposes.

REFERENCES

Astridge, D.G.: Vibration Health Monitoring of the Westland 30 Helicopter Transmission—Development and Service Experience. Detection, Diagnosis, and Prognosis of Rotating Machinery to Improve Reliability, Maintainability, and Readiness through the Application of New and Innovative Techniques, T.R. Shives and L.J. Mertaugh, eds., Cambridge University Press, New York, 1988, pp. 200–215.

Braun, S.: Mechanical Signature Analysis—Theory and Applications. Academic Press, New York, 1986.

Braun, S.; and Datner, B.: Analysis of Roller/Ball Bearing Vibrations. Mech. Des., vol. 101, Jan. 1979, pp. 118–125.

Cempel, C.: Vibroacoustical Diagnostics of Machinery: An Outline. Mech. Syst. Signal Proces., vol. 2, no. 2, 1988, pp. 135–151.

Childers, D.G.; Skinner, D.P.; and Kemerait, R.C.: The Cepstrum: A Guide to Processing. Proc. IEEE, vol. 65, no. 10, Oct. 1977, pp. 1428–1443.

Chin, H.; and Danai, K.: Fault Diagnosis of Helicopter Power Trains. Proceedings of the 17th Annual National Science Foundation Grantees Conference in Design and Manufacturing Systems Research, Society of Manufacturing Engineers, Dearborn, MI, 1991, pp. 787–790.

Chow, E.Y.; and Willsky, A.S.: Analytical Redundancy and the Design of Robust Failure Detection Systems. IEEE Trans. Autom. Control, vol. AC–29, no. 7, July 1984, pp. 603–614.

Collier-March, A.: Operational Experience with the Advanced Transmission Health Monitoring Techniques on the Westland 30 Helicopter. Presented at the 11th European Rotorcraft Forum, 1985, Paper 43.

Courrech, J.; and Gaudet, M.: Envelope Analysis—the Key to Rolling-Element Bearing Diagnosis. Bruel & Kjaer Application Notes, a Pamphlet, Larcenk & Sons, Denmark, 1985.

Danai, K.; and Chin, H.: Fault Diagnosis with Process Uncertainty. J. Dyn. Syst. Measur. Control, vol. 113, no. 3, Sept. 1991, pp. 339–343.

Dewell, D.L.; and Mitchell, L.D.: Detection of a Misaligned Disk Coupling Using Spectrum Analysis. J. Vib. Acoust. Stress Reliab. Design, vol. 106, Jan. 1984, pp. 9–16.

Dyer, D.; and Stewart, R.M.: Detection of Rolling Element Bearing Damage by Statistical Vibration Analysis. J. Mech. Des., vol. 100, Apr. 1978, pp. 229–235.

Hertz, J.; Krogh, A.; and Palmer, R.G.: Introduction to the Theory of Neural Computation. Addison-Wesley, Redwood City, CA, 1991.

Kaufman, A.B.: Measure Machinery Vibration—It Can Help You Anticipate and Prevent Failure. Instrum. Control Syst., vol. 48, Feb. 1975, pp. 59–62.

Lees, A.W.; and Pandey, P.C.: Vibration Spectra from Gear Drives. Second International Conference on Vibration in Rotating Machinery, Mechanical Engineering Publications, London, UK, 1980, pp. 103–108.

Lewicki, D.G.; Decker, H.J.; and Shimski, J.T.: Full-Scale Transmission Testing to Evaluate Advanced Lubricants. NASA TM–105668, 1992.

Ljung, L.: System Identification: Theory for the User. Prentice-Hall, Inc., Englewood Cliffs, NJ, 1987.

Lyon, R.H.; and Ordubadi, A.: Use of Cepstra in Acoustical Signal Analysis. J. Mech. Des., vol. 104, Apr. 1982, pp. 303–306.

Mathew, J.; and Alfredson, R.J.: The Condition Monitoring of Rolling Element Bearings Using Vibration Analysis. J. Vib. Acoust. Stress Reliab. Des., vol. 106, July 1984, pp. 447–453.

McFadden, P.D.; and Smith, J.D.: A Signal Processing Technique for Detecting Local Defects in a Gear From the Signal Average of the Vibration. Proc. Inst. Mech. Eng., vol. 199, no. C4, 1985, pp. 287–292.

Mertaugh, L.J.: Evaluation of Vibration Analysis Techniques for the Detection of Gear and Bearing Faults in Helicopter Gearboxes. Detection, Diagnosis, and Prognosis of Rotating Machinery to Improve Reliability, Maintainability, and Readiness through the Application of New and Innovative Techniques, T.R. Shives and L.J. Mertaugh, eds., Cambridge University Press, New York, 1988, pp. 28–30.

Pau, L.F.: An Adaptive Signal Classification Procedure Application to Aircraft Engine Condition Monitoring. Pattern Recog., vol. 9, 1977, pp. 121–130.

Pratt, J.L.: Engine and Transmission Monitoring—A Summary Promising Approaches. Detection, Diagnosis, and Prognosis of Rotating Machinery to Improve Reliability, Maintainability, and Readiness through the Application of New and Innovative Techniques, T.R. Shives and L.J. Mertaugh, eds., Cambridge University Press, New York, 1988, pp. 229–236.

Randall, R.B.: A New Method of Modeling Gear Faults. J. Mech. Des., vol. 104, Apr. 1982, pp. 259–267.

Rumelhart, D.E.; Hinton, G.E.; and Williams, R.J.: Learning Error Representation by Error Propagation. Parallel Distributed Processing—Explorations in the Microstructure of Cognition, Vol. 1: The Foundations, D.E. Rumelhart and J.L. McClelland, eds., MIT Press, Cambridge, MA, 1988.

MSDA User's Guide. Stewart Hughes Limited, Southampton, UK, 1986.

Taylor, J.I.: Identification of Bearing Defects by Spectral Analysis. J. Mech. Des., vol. 102, Apr. 1980, pp. 199–204.

Yhland, E.; and Johansson, L.: Analysis of Bearing Vibration. Aircr. Eng., vol. 42, Dec. 1970, pp. 18–20.

REPORT DOCUMENTATION PAGE	Form Approved OMB No. 0704-0188

1. AGENCY USE ONLY (Leave blank)	2. REPORT DATE April 1993	3. REPORT TYPE AND DATES COVERED Technical Memorandum

4. TITLE AND SUBTITLE

Fault Detection of Helicopter Gearboxes Using the
Multi-Valued Influence Matrix Method

5. FUNDING NUMBERS

WU-505-63-36
1L162211A47A

6. AUTHOR(S)

Hsinyung Chin, Kourosh Danai, and David G. Lewicki

7. PERFORMING ORGANIZATION NAME(S) AND ADDRESS(ES)

NASA Lewis Research Center
Cleveland, Ohio 44135-3191
and
Propulsion Directorate
U.S. Army Aviation Systems Command
Cleveland, Ohio 44135-3191

8. PERFORMING ORGANIZATION REPORT NUMBER

E-7742

9. SPONSORING/MONITORING AGENCY NAMES(S) AND ADDRESS(ES)

National Aeronautics and Space Administration
Washington, D.C. 20546-0001
and
U.S. Army Aviation Systems Command
St. Louis, Mo. 63120-1798

10. SPONSORING/MONITORING AGENCY REPORT NUMBER

NASA TM-106100
AVSCOM TR-92-C-015

11. SUPPLEMENTARY NOTES

Hsinyung Chin and Kourosh Danai, Department of Mechanical Engineering, University of Massachusetts, Amherst, Massachusetts 01003 and David G. Lewicki, Propulsion Directorate, U.S. Army Aviation Systems Command. Responsible person, David G. Lewicki, (216) 433-3970.

12a. DISTRIBUTION/AVAILABILITY STATEMENT

Unclassified - Unlimited
Subject Category 37

12b. DISTRIBUTION CODE

13. ABSTRACT (Maximum 200 words)

In this paper we investigate the effectiveness of a pattern classifying fault detection system that is designed to cope with the variability of fault signatures inherent in helicopter gearboxes. For detection, the measurements are monitored on-line and flagged upon the detection of abnormalities, so that they can be attributed to a faulty or normal case. As such, the detection system is composed of two components, a *quantization matrix* to flag the measurements, and a *multi-valued influence matrix* (MVIM) that represents the behavior of measurements during normal operation and at fault instances. Both the *quantization matrix* and *influence matrix* are tuned during a training session so as to minimize the error in detection. To demonstrate the effectiveness of this detection system, it was applied to vibration measurements collected from a helicopter gearbox during normal operation and at various fault instances. The results indicate that the MVIM method provides excellent results when the full range of faults effects on the measurements are included in the training set.

14. SUBJECT TERMS

Influence coefficients; Diagnosis; Failure analysis; Transmissions (machine elements)

15. NUMBER OF PAGES
30

16. PRICE CODE
A03

17. SECURITY CLASSIFICATION OF REPORT	18. SECURITY CLASSIFICATION OF THIS PAGE	19. SECURITY CLASSIFICATION OF ABSTRACT	20. LIMITATION OF ABSTRACT
Unclassified	Unclassified	Unclassified	